



**HAL**  
open science

## New experimental approach to accelerate the development of internal swelling reactions (ISR) in massive concrete structures

Jacques Jabbour, Aveline Darquennes, Loic Divet, Rachid Bennacer, Jean-Michel Torrenti, Georges Nahas

### ► To cite this version:

Jacques Jabbour, Aveline Darquennes, Loic Divet, Rachid Bennacer, Jean-Michel Torrenti, et al.. New experimental approach to accelerate the development of internal swelling reactions (ISR) in massive concrete structures. *Construction and Building Materials*, 2021, 313, pp.125388. 10.1016/j.conbuildmat.2021.125388 . hal-04274364

**HAL Id: hal-04274364**

**<https://cnrs.hal.science/hal-04274364v1>**

Submitted on 5 Jan 2024

**HAL** is a multi-disciplinary open access archive for the deposit and dissemination of scientific research documents, whether they are published or not. The documents may come from teaching and research institutions in France or abroad, or from public or private research centers.

L'archive ouverte pluridisciplinaire **HAL**, est destinée au dépôt et à la diffusion de documents scientifiques de niveau recherche, publiés ou non, émanant des établissements d'enseignement et de recherche français ou étrangers, des laboratoires publics ou privés.



Distributed under a Creative Commons Attribution - NonCommercial 4.0 International License

## New experimental approach to accelerate the development of internal swelling reactions (ISR) in massive concrete structures

Jacques Jabbour<sup>a,b,c\*</sup>, Aveline Darquennes<sup>b</sup>, Loïc Divet<sup>c</sup>, Rachid Bennacer<sup>b</sup>, Jean-Michel Torrenti<sup>c</sup>, Georges Nahas<sup>a</sup>

<sup>a</sup> IRSN, Fontenay-aux-Roses, France

<sup>b</sup> LMT ENS-Paris-Saclay, CNRS, University Paris-Saclay, Cachan, France

<sup>c</sup> University Gustave Eiffel, IFSTTAR, F-77447 Marne la Vallée, France

---

### Abstract

Internal Swellings Reactions (ISR) are pathologies that are likely to degrade concrete by causing swelling, cracking and major disorders in structures. Many laboratory studies of internal swelling reactions are realized on relatively small size samples. Those laboratory samples do not allow to replicate real conditions to which the real concrete is submitted in its environment, in terms of aging kinetics, ionic transport, early age thermal history and mechanical conditions especially in massive structures. Therefore, an experimental approach to accelerate internal swelling reactions of concrete at the structure scale is developed to allow better observation and understanding of swelling reactions at a massive structure scale. Two representative massive concrete structures (2.4 x 1.4 x 1 m<sup>3</sup>) were realized under controlled and optimized conditions for the development of alkali-silica reaction (ASR) and delayed ettringite formation (DEF). An instrumentation system is developed thus allowing to monitor evolutions of the pathologies in the massive structures both internally and externally. The respective deformations and cracking were tracked for over 3 years. Results show different swelling kinetics and amplitudes among the mock-ups and allow validating the proposed approach. Expansions in massive structures vary greatly from analogous laboratory samples. Boundary conditions and confinement effects could hinder swelling along certain directions thus compensated by a higher expansion along unstressed directions which leads to an anisotropic behavior in the material and impacts the cracking orientation. Residual swelling tests reveal the chemical potential of the internal swelling reactions and define an upper strain limit for the structure. They reveal as well a scale effect on the reactional kinetics and on the swelling amplitude.

*Keywords:* Concrete degradation, massive structure, internal swelling reactions, alkali-silica reaction, delayed ettringite formation, kinetics, accelerated aging, multi-scale, test method.

## 1. Introduction

The work described in this article is part of a research program on the aging of nuclear infrastructures launched by the IRSN (Institute for Radiological Protection and Nuclear Safety) in the context of the French operator EDF's intention to extend the lifespan of the French nuclear power plants. The goal is to contribute to the knowledge of aging mechanisms touching the constituents of non-replaceable structures of a nuclear power plant, such as the containment building. As a matter of fact, such structures play an important role for safety as they mainly constitute the third and last barrier against the dispersion of radioactive particles in the environment. Among the phenomena involved in aging mechanisms, internal swellings reactions are pathologies likely to degrade concrete by causing swelling, cracking and major disorders in the affected structures. They include the delayed ettringite formation (DEF) and the alkali-silicate reaction (ASR). These pathologies are endogenous reactions, occurring as a result of the interaction between the initial components of the material. These interactions take place following the use of reactive aggregates in case of ASR or following a significant warm-up at early age of the concrete in case of DEF. In nuclear facilities, the possibility of seeing these phenomena develop cannot be ruled out as they affect in priority massive reinforced concrete elements for which a significant heating could have occurred at the early age and reactive aggregates may in some cases have been used during the construction phase. Therefore those risks ought to be studied and quantified especially for mastering the safety of these facilities in the context of their lifetime extension [1].

The kinetics of these reactions is generally slow and it can take up to a few decades for disorders to appear in the structure [2] [3]. Among the solutions used in research laboratories to study these pathologies, one is to use accelerated test methods developed on small specimens [2] [3] [4]. The size of laboratory samples makes it easier to accelerate diffusive phenomena, however they do not allow to reproduce real conditions to which the real concrete is submitted in its environment, in terms of volume/surface

65 ratio and thermal conditions especially in massive structures. Different accelerated tests  
have been proposed in the literature in order to assess the reactive potential of mortars  
or concretes with regard to the delayed formation of ettringite or the alkali-aggregate  
reaction prior to adopting them for construction purposes [3] [4] [5]. Most of these tests  
70 are essentially based on pre-damage to the test specimens (by freeze-thaw cycles or by  
drying/humidification cycles) or on very high heat treatments. These tests are open to  
criticism, on the one hand, due to the high temperatures imposed repeatedly on samples  
whose dimensions remain small and, on the other hand, as to the nature of the initial  
damage. Therefore, classic laboratory tests do not allow a realistic observation of these  
pathologies in massive structures. Hence, this article will focus on the development and  
75 validation of an experimental approach to accelerate internal swelling reactions of  
concrete on a massive structural scale to allow better observation and understanding of  
these pathologies. First, the chosen materials and mock-ups description are presented.  
Then, an acceleration strategy specific to each internal swelling reaction is developed  
and the mock-ups' manufacturing process, conservation environment and experimental  
80 program are detailed. Finally, the evolution of these pathologies in the different mock-  
ups are measured and analyzed.

## 2. Mock-ups description and materials

The mock-ups built are 2.4 meters long, 1.4 meters high and 1 meter thick. The  
dimensions choice is due to logistical constraints in order to allow the handling and  
85 manufacture of these massive samples. However, the thickness of one meter is the  
desired dimension, representative of the structures of interest, and considered to be  
scale 1 for this study. These are non-reinforced concrete elements. The concrete mixes  
chosen for each of the mock-ups were selected so that their chemical composition is  
favorable to the development of the pathologies. They consist of a Portland cement  
90 CEM II/A-LL 42.5 R, of aggregates having three granular sizes: 0-5 mm (sand), 5-12.5  
mm and 12.5-20 mm (gravel), a water to cement ratio (W/C) of 0.57 and a water  
reducing plasticizer. The mass proportions and the granular curves of the aggregates  
are identical for both mock-ups; however the origin of the aggregates varies. The  
concrete mix C1 used in this study is given in Table 1 and the chemical and  
95 mineralogical compositions of the cement are given in Tables 2 and 3.

**Table 1:** Concrete mix C1 proportions

	Weight (Kg/m <sup>3</sup> )
Cement CEM II A-LL 42.5 R	400
Sand 0/5	772
Coarse aggregates 5/12.5	316
Coarse aggregates 12.5/20	784
Water	228
Plasticizer	1.4

**Table 2:** Chemical analyses of cement CEM II/A-LL 42.5 R.

	Wt. %
SiO <sub>2</sub>	19.37
Al <sub>2</sub> O <sub>3</sub>	4.58
Fe <sub>2</sub> O <sub>3</sub>	3.06
TiO <sub>2</sub>	0.28
MnO	0.07
CaO	63.66
CaO	63.66
MgO	1.30
SO <sub>3</sub>	2.87
K <sub>2</sub> O	1.50
Na <sub>2</sub> O	0.07
P <sub>2</sub> O <sub>5</sub>	0.50
Na <sub>2</sub> O <sub>eq</sub>	1.06
S <sub>2-</sub>	<0.02
Cl <sub>2-</sub>	0.03

100

**Table 3:** Mineralogical composition of cement CEM II/A LL 42.5 R

	Wt. %
C <sub>3</sub> S	65.7
C <sub>2</sub> S	9.8
C <sub>3</sub> A	7.4
C <sub>4</sub> AF	11.4

The aggregates used for the DEF mock-up are limestone aggregates from the Pays de Loire region (France) (0/20 mm). Whereas, for the ASR mock-up, the sand (0/5 mm) is a non-reactive calcareous sand from the Boulonnais region (France) and the gravel (5/20 mm) comes from the Tournaisis region (Belgium) comprising a diffuse silica network (reactive aggregates PR) [6]. The characteristics of the aggregates used in this study are given in Table 4.

**Table 4:** Mineralogical composition of cement CEM II/A LL 42.5 R

	<i>DEF mock-up</i>		<i>ASR mock-up</i>	
	Type	Absolute Density (Kg/m <sup>3</sup> )	Type	Absolute Density (Kg/m <sup>3</sup> )
<b>Sand 0/5</b>	NR, calcareous	2704	NR, calcareous	2710
<b>Coarse aggregates 5/12.5</b>	NR, calcareous	2676	PR, silicious	2669
<b>Coarse aggregates 12.5/20</b>	NR, calcareous	2680	PR, silicious	2664

### 3. DEF mock-up acceleration strategy

The main parameters influencing the kinetics of DEF, apart from those relating to the composition of the concrete, are: the amount of destabilized ettringite due to the thermal conditions at the early age and the conservation environment (notably the presence of water and the leaching of alkalis). Therefore the intuitive strategy to accelerate this pathology in the dedicated mock-up would be to optimize those two parameters.

The cement used have a composition satisfying the conditions for developing the pathology (aluminates to sulfate ratio equals to 0.7, equivalent sodium content equals to 1,06% of the cement mass), hence the early-age thermal profile of the structure becomes the key factor for initiation of the reaction. In order to optimize this parameter, the quantity of delayed ettringite formed is maximized as a function of the heat treatment applied by means of a numerical simulation. Several types of models exist in the literature to describe the DEF reaction [7][8][9]. These models have varying degrees of complexity and precision in reproducing the reaction mechanisms of DEF. Complete numerical models at the grain level evoke several multi-physical parameters (thermo-

hydro-chemo-mechanical) that are difficult to identify [7]. Subsequently, we opted for an empirical model linking the amount of ettringite formed to the content of sulfates, aluminates, alkalis as well as to the heat treatment applied [10]. This model reveals a parameter called "EU" ("effective thermal energy" expressed in °C.hr) integrating the concrete's temperature above 65 °C during the corresponding time (in hours) causing the destabilization of ettringite at the early age and its precipitation later [10] given in Equation 1.

$$Effective\ thermal\ Energy\ (EU) = \begin{cases} \int (T(t) - 65)dt & \text{if } T(t) > 65^{\circ}C \\ 0 & \text{else} \end{cases} \quad (Eq. 1)$$

The parameters of this model are identified based on the concrete's composition and thanks to a swelling database for known heat treatments applied to this concrete.

Figure 1 presents the evolution of an ettringite indicator (I\_Aft) corresponding to this phenomena and specific to this concrete mix. It is noted that the indicator of ettringite formation increases with EU, up to a value of approximately 1500 °C.hr from which it decreases. The decreasing part of the curve, also known as the "pessimum effect", corresponds to the fact that the amount of free aluminates becomes insufficient to react with the sulfates in order to form ettringite. This is due to the increase of the final adsorption of the aluminates on the C-S-H structure with the increase in the duration of the heat treatment by substitution of the silicates (Si) thus forming siliceous hydrogrenates (HGSI, C-AS-H or CAH). This final adsorption results in the fall of the aluminates to sulfates ratio thus limiting the differed precipitation of ettringite [7][10].

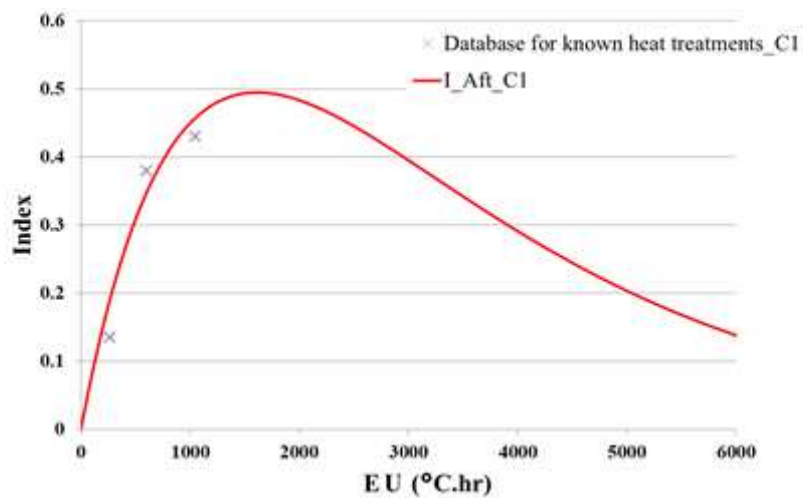


**Figure 1: Evolution of the ettringite indicator (I\_Aft\_B11) in red, function of the early-age heat treatment (EU)**

Certainly, this semi-empirical model has limits as to the precision of the mechanisms reproduced. However, it provides a quick tool for deciding on the relevance of a given heat treatment with regard to the development of DEF. Thus it is shown that for this concrete mix, the effective thermal energy (EU) necessary to maximize the amount of destabilized ettringite (therefore present in the system) is approximately 1500 °C.hr. It can be obtained by several early age heat treatments: conservation at 70 °C for 12 days (300 hours), at 80 °C for 4 days (100 hours), at 90 °C for 60 hours, etc. In practice, a long-term heat treatment is complex to implement and is also likely to reduce the final expansion of the concrete. A heat treatment at very high temperatures (such as 80-90 °C) is likely to change the nature of hydrates [4]. Taking these observations into account, the heat treatment chosen for the DEF mock-up consists of maintaining the temperature at 80 °C (deemed less penalizing than 90°C) for 100 hours.

From another perspective, in the case of massive structures there is often a large temperature gradient between the core and the skin. The core temperature eventually exceeds 65 °C due to the exothermic hydration reactions, while at the edges the temperature is closer to room temperature which leads to the creation of a field of non-homogeneous ettringite formation in the mass, as shown by the models of [8]. This phenomenon, combined with the fact that the environmental conditions act mainly on the concrete surface (such as the leaching of alkalis) are part of the factors explaining the long latency times before the manifestation of DEF in massive structures. In order to reverse this trend and reduce the latency time, the idea is to eliminate this temperature gradient and ensure a homogeneous thermal profile within the volume of the DEF mock-up. By doing so, it is expected that the pathology will first appear on the surface and progress to the heart knowing that the leaching of the alkalis will act first at the concrete skin.

As for the mock-up storage conditions, they have a significant but complex influence on swellings due to DEF in terms of amplitude and kinetics. Several studies have shown that the conservation temperature influences the amplitude and the kinetics of the concrete's expansions [11] [12]. Thus, a high storage temperature (38°C) is unfavorable with regard to the final amplitude of the expansion, but accelerates its kinetics in comparison with a storage temperature of 23 °C [11]. The weak expansions observed



at a high storage temperature can be explained by the increase in the solubility of ettringite, which can cause lower crystallization pressures within the material. The acceleration of the kinetics is due to the increase in the rates of ionic transfers at the level of the porous matrix. Eventually, a storage temperature of  $20 \pm 2$  °C is identified as a good compromise for the DEF mock-up.

From a hydric point of view, the influence of water on ISR development is widely observed [11][12]. In the course of the reactions, water has two functions: a reactant function; the available quantities affecting the amplitude of the swellings; and a reaction medium function by allowing the ionic transport and therefore bringing the reactants into contact. Relative Humidity (RH) threshold values have been identified in the context of various studies, whether for ASR ( $80 \leq RH \leq 100\%$ ) or for DEF ( $92\% \leq RH \leq 100\%$ ) [12] [13][14]. The choice falls on a complete immersion of both mock-ups, thus facilitating the maintenance of a controlled hydric atmosphere. In the case of the DEF mock-up, submerging the structure also increases alkalis leaching which highly increases the reaction's kinetics as well.

In summary, the strategy adopted to accelerate DEF in the allotted mock-up consists of the following measures:

- Apply an early-age heat treatment of 80°C during 100 hours and ensure a homogeneous temperature profile within the structure's volume.
- Conserve the mock-up at 20°C fully immersed in water
- Change regularly the conservation water in order to allow for external observations but also to increase alkali leaching.

#### **4. ASR acceleration strategy**

Three elements are essential for the development of the alkali-silica reaction: alkalis, reactive silica and water. If we apply the previous approach to accelerate the swelling in the mock-up dedicated to study the ASR, it amounts to: maximizing both the amount of reactive silica and the concentration of alkalis available in the system, and to determine the optimal temperature to maintain. This methodology is carried out while avoiding pre-damage to the studied structure, whether of thermal, mechanical or hydric origin.

The sizes of the reactive aggregates, their distribution and the nature of the reactive silica have an important influence on the intensity of the reaction [15]. The granular combination (non-reactive sand + reactive aggregates) is chosen based on the works of Guedon-Dubied [4], hence the same quarry provides the reactive aggregates. These aggregates are rich in amorphous silica having the texture and composition of chalcedony and opal which, from a mineralogical point of view, is deemed to have a significant alkali reactivity [6]. Furthermore, Monnin showed that the kinetics of alkali consumption increases when the aggregate diameter decreases [16]. This causes a rapid drop in the alkali concentration of the interstitial solution which may limit the final swelling of the concrete. Therefore, by opting for non-reactive sand, the final swelling due to the alkali-granulate reaction is maximized. The binder used contains 1.06% of Na<sub>2</sub>eq (by mass), hence providing a total of 4.24 Kg/m<sup>3</sup> of alkalis in the mix. As a result, this concrete mix is highly ASR-prone.

As for the storage conditions, temperature has a preponderant effect on the kinetics of the alkali-silica reaction and is being used in numerous laboratory experiments [17]. At ambient temperature ASR takes several years before manifesting and requires several decades for swelling to stabilize. At high temperatures, the reaction is accelerated and the deformations appear quickly. Thus by conserving the concrete at 38 °C, the swelling begins immediately, while it is necessary to wait longer at 23 °C [17]. From a theoretical point of view, an increase in temperature causes a decrease in the solubility of portlandite and an increase in that of silica, which should result in an aggravation of the disorders. Therefore, a temperature of 38 °C is determined to be optimal for the conservation of the mock-up in order to favor the development of ASR.

By reasoning in a similar fashion to the DEF acceleration strategy, and by taking into account the influence of water on the development of ISR and its functional roles (reactant + reaction medium), the ASR mock-up is submerged in a pool and maintained at 38 ± 2 °C. The pool is emptied at the same frequency as the pool containing the DEF mock-up in order to allow the macroscopic monitoring of the structure. Even though this choice leads to alkali leaching, which is counter-intuitive in the case of ASR, however it is retained for practical reasons. Moreover, in order not to couple ASR with DEF in this mock-up, a criterion limiting the maximum early-age temperature to 62° C is fixed.

## 5. Mock-ups instrumentation

240 The monitoring methods used are intended to track the behaviour of the concrete  
from its early age until the swellings' stabilization. Three main parameters are retained:  
the thermal history and the temperature's distribution in the mock-up's volume  
(especially at the early age), the internal swelling and the external cracking of the  
structure. As a result, a suitable instrumentation system is designed.

245 A cross section of the mock-up is instrumented with 16 Type J thermocouples as  
shown in Figure 2. This makes it possible to follow the evolution of the temperature  
during the hydration of the cement, the thermal gradient in the concrete in both  
directions and the temperature variations during the test following the surrounding  
conditions.

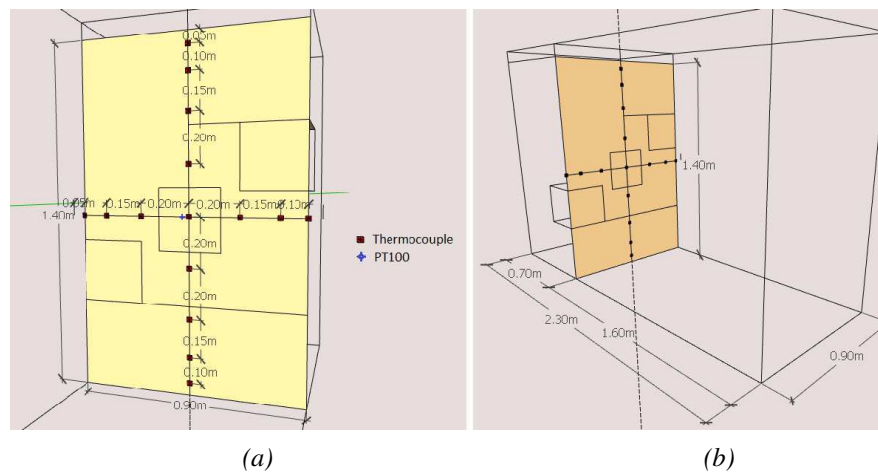


**Figure 2 : (a) cross section and (b) perspective view of the support showing the positioning of the thermocouples**

250 The monitoring of swelling in the structure is ensured by 3 strain gauge rosettes R1,  
R2 and R3 located respectively at three levels: the top ( $3H/4$ ), the center ( $H/2$ ) and  
at the bottom ( $H/4$ ) of the mock-up, where  $H$  is the mock-up height (140 cm). Each rosette  
is constituted of three vibrating wire extensometers that are oriented in three directions  
(X, Y and Z) making it possible to continuously follow the deformations over time with  
255 an accuracy of the order of  $2 \mu\text{m/m}$ .

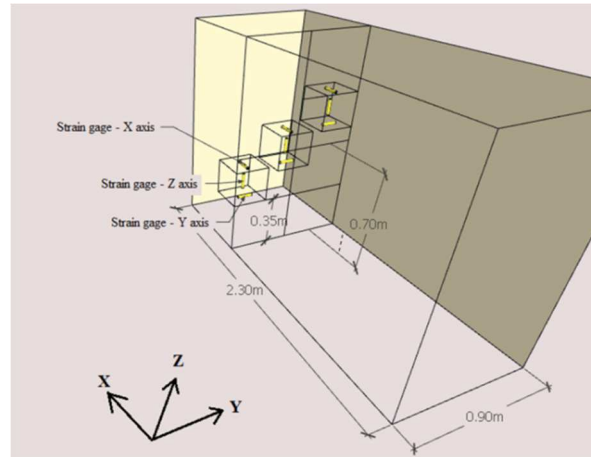


**Figure 3: Strain sensors placement in the structure (dimensions not including concrete cover)**

Knowing that the introduction of embedded devices (including the associated cables) could be considered intrusive with regard to the concrete, instrumentation is limited to one third of the mock-up. As a result, an area without instrumentation, roughly equivalent to two thirds of the mock-up, is provided in order not to hinder the swelling  
 260 in the raw concrete and to allow coring thereafter.

An advantage of constructing mock-ups of such dimensions is the possibility to conduct macroscopic monitoring using proven industrial methods. Thus, the determination of the cracking index of a concrete surface according to the LPC n °47 test method is applicable to monitor the state of degradation of the mock-ups over time  
 265 [18]. The cracking index represents an average crack opening (in mm) per square meter of concrete ( $m^2$ ). This method is usually used to characterize in a simple and rapid manner the state of degradation of a concrete structure suffering from swelling pathology. Thus, the surface of the none-instrumented zone of the mock-up is chosen for this purpose. Figure 4 features the axis/area used to monitor the cracking index of the DEF mock-up and the mock-up's state prior to applying the accelerated aging  
 270 strategy.



**Figure 4: the axis/area used to monitor the cracking index of the DEF mock-up**

## **6. The early-age heat treatment of the mock-ups**

In order to successfully realize the mock-ups in accordance with the established acceleration strategies, it is essential to master their thermal profiles at the early age of the concrete because it's a key factor for the initiation of the swelling pathologies. Given the size of the mock-ups ( $2.4 \times 1.4 \times 1 \text{ m}^3$ ), the adopted methodology to control their thermal profile is as follows: first, characterize the temperature rise in the structures due to the heat generated by the hydration of cement then select and manoeuver levers in order to obtain the desired thermal profiles: maximum temperature  $T_{\text{max}}$  below  $62^\circ\text{C}$  in the ASR mock-up and  $T_{\text{max}} \approx 80^\circ\text{C}$  for 100 hours in the DEF mock-up.

In order to predict the heat released due to the hydration of the cement in these massive structures, several elements are identified:

- o The hydration reaction of the cement
- o The thermal transfers between the mock-ups and their environment (exchange coefficients with the exterior)
- o The thermo-chemical parameters related to the cement and the concrete formulation (chemical affinity and cement dosage).

290 These elements are then implemented in a finite elements simulation which made it possible to carry out a parametric study to assess the sensitivity of these parameters and anticipate their variability [19] [20]. The levers selected to adjust the thermal profile of the mock-ups are the initial temperature of the concrete as well as the thermal properties of the formwork (boundary conditions).

295 In the ASR case, an initial concrete temperature of 20 °C is found optimal in order to remain below 62°C at the peak of the temperature rise. Whereas in the DEF case, it is found optimal to start from 35 °C in order to reach the 80°C objective. The concrete ingredients are either cooled or heated prior to mixing and multiple blank tests are realized in order to target the required initial temperatures once the concrete is placed in the formworks. The thermal gradients between the mockups' core and extremities  
300 are also evaluated because they can generate significant mechanical stresses and a risk of cracking at early-age. Since these massive structures are not reinforced, a criterion limiting the thermal gradient to 10°C is defined based on the mechanical performance of concrete at 1 day. As a matter of fact, early-age thermal cracking occurs when the tensile strain, arising from either restrained thermal contraction or a temperature  
305 differential within the concrete section, exceeds the tensile strain capacity of the concrete. A 10 cm thick glass wool insulation is added to the formworks in order to limit the temperature gradient and prevent from thermal cracking. The steel formworks are loosened directly after the hardening of concrete as well. Figure 5 features the temperature profile of the ASR mock-up at various depths.

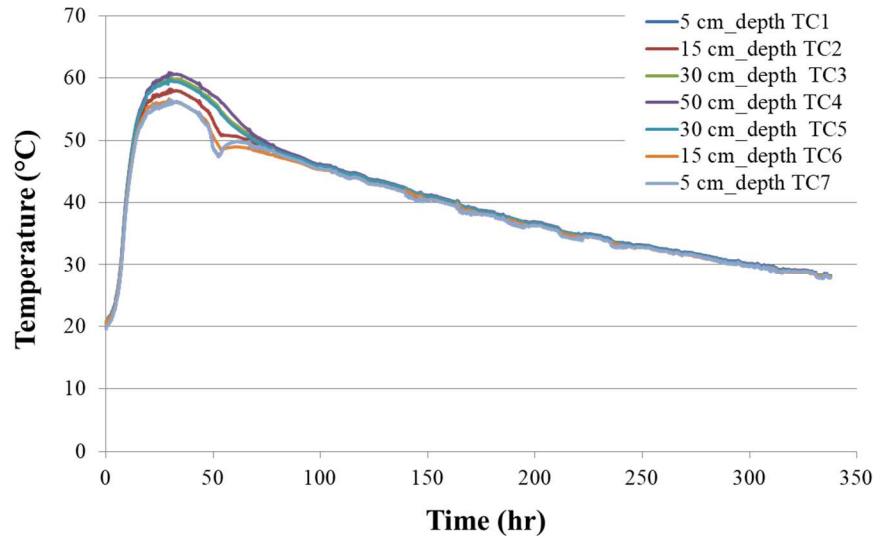


**Figure 5 : Early-age thermal profile of the ASR mock-up**

310 The objectives of not exceeding 62°C and limiting the thermal gradient to 10°C in order to prevent cracking are assured. At t = 72 hours, the mock-up's formwork is stripped down to allow the production of the DEF mock-up. The thermal insulation is restored briefly after. This explains the temporary drop in the skin temperature.

315 The heat treatment of the DEF mock-up is assured by adding a heating skin containing thermal resistances and glued to the surface of the metal formwork. Once the concrete reaches 80°C at the core of the mock-up, the heating skin is activated. Its role is only to compensate for heat losses in order to maintain the whole mock-up at 80 ° C for 100 hours and to cool it gradually thereafter. This heating skin is controlled by a temperature probe placed 10 cm deep in the concrete. The operating mode is chosen  
 320 so as not to exceed the set temperature during the regulation phase. In this way the temperature is homogeneous in the block (figure 7). Figure 6 shows the heating skin and its control system.



**Figure 6 : DEF mock-up's early-age temperature regulation system**

Figure 7 features the temperature profile of the DEF mock-up at various depths.

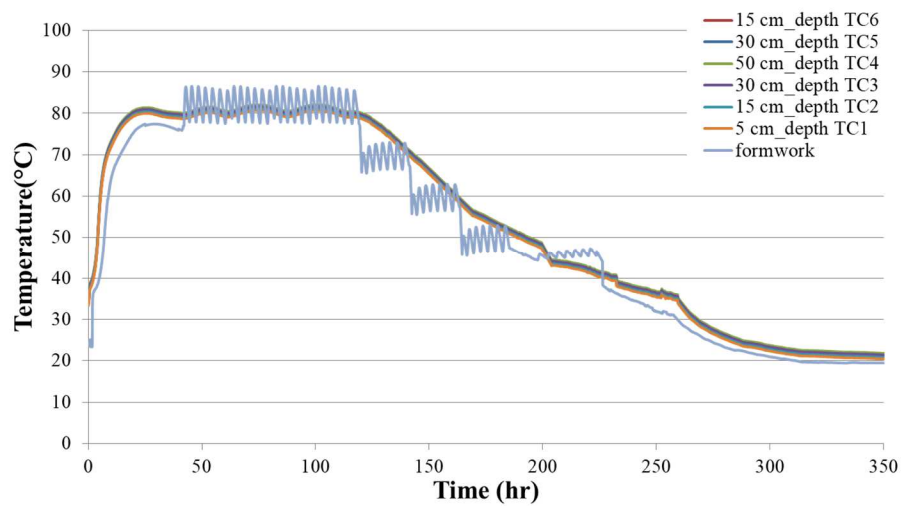


**Figure 7 : Early-age thermal profile of the DEF mock-up**

325 Slight variations during the 80 °C plateau are observed, they are due to the day/night temperature variation and to the fact that the mock-up have been exposed to solar radiations.

## 7. The mock-ups' manufacturing process

The mock-ups are manufactured in an industrial platform hence providing a controlled environment (average temperature = 19 °C, average relative humidity =



330 70%). Afterwards, they are transported by truck to be installed in their respective pools  
built specifically for the sake of this study.

The manufacturing process is done in several stages. First, convenience tests are  
carried out in order to set-up an efficient work chain methodology and to optimize the  
temperature of fresh concrete. Subsequently, several blank castings are carried out over  
335 several consecutive days under real conditions in order to optimize the heating of  
aggregates and the concrete's rheology. Feedback shows that aggregates must be  
conditioned to around 55 °C and water must be heated to 60 °C in order to obtain 35 °C  
once the concrete is placed in the formwork and vibrated. This is due to heat losses  
during handling and mixing. It has also been found that the concrete's rheology at 35°C  
340 is not identical at 20 °C. This is due to a faster hydration rate of the cement as well as  
greater absorption rate of water from the hot aggregates. To remedy this, the  
actual/heated absorption coefficients are measured and the amount of superplasticizer  
is adjusted to ensure a slump of 18 cm in order to preserve the instrumentation and  
facilitate the placement of the concrete.

345 Before the concrete mixing starts, the bottom of the formwork is thermally insulated  
(Figure 8) and the formwork is well lubricated, then the system used to support the  
instrumentation is delicately placed inside. The mock-ups' metal support (bottom of the  
formwork) consists of a metal plate welded to I-section steel beams. It is designed to  
allow for the handling of these structures in a manner that the tensile stress in the mock-  
up doesn't exceed 1 MPa while lifting. Concrete is simply poured on top of this support  
350 and after the concrete hardens, the support becomes part of the mock-up.

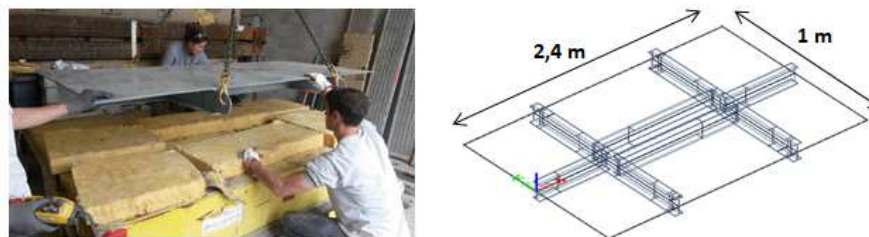


**Figure 8: The mock-ups' metal support (bottom of the formwork)**

The casting of each mock-up is carried out in 10 successive batches of 400L each.  
Each layer of concrete is vibrated in a way that the previous layer is penetrated for about

5 cm by the vibrating needle. This is to ensure the homogeneity of the block. The total  
355 time for casting a mock-up is 2 hours 30 minutes from the time water is added to the  
first batch and until the vibration of the last layer. Concrete samples are taken from each  
batch in order to confirm compliance with the mechanical specifications of the concrete.  
Some samples are made up of two concrete lifts from two successive batches in order  
to test the homogeneity between the different layers. The results of the mechanical tests  
360 are in accordance with the specifications. Compression tests at 28 days and 90 days,  
porosity accessible to water, static and dynamic Young's modulus, splitting and bending  
tests are carried out. The compressive strength obtained at 28 days is around 40 MPa,  
in accordance with the target value.

Special measures are taken to prevent the DEF mock-up from drying while  
365 undergoing the early-age heat treatment. Thus, a reduced flow of hot water (around  
60°C) constantly submerged the upper surface of the concrete throughout the heat  
treatment. At the end of the early-age heat treatment, the formworks are disassembled  
and the axis' used for monitoring the crack index are drawn. Then the mock-ups are  
wrapped using plastic film (Figure 9) to avoid drying and loaded for transportation to  
370 their storage environment. (Figure 10)



**Figure 9 : Mock-up wrapped in plastic film**



**Figure 10 : Loading of the mock-up using a crane and the metal bottom support**

## **8. The mock-ups' conservation environment**

An experimental platform is built to accommodate these massive structures in a controlled conservation environment. The mockups are placed in their respective pools before the roofs are assembled (Figure 11). Each pool is 3.9 meters in diameter and 2 meters in height. The water level is 1.8 meter. Each basin therefore contains a total volume of water of 18.7 m<sup>3</sup>. The basin containing the ASR mock-up is maintained at 38°C (± 2°C) whereas the basin containing the mock-up is kept at 20°C (± 2°C). For each cycle, the pools' water is gradually heated in order to reach the target conservation temperature for each mock-up, then the mock-ups are kept at constant temperature for 28 consecutive days, and afterwards they are gradually cooled before the pools are emptied to allow for macroscopic observations. In fact, the cycle's duration is optimized with regard to the leaching of alkalis but also from an economic and ecological point of view, given that a basin contains an important volume of water renewed cyclically. The transition between two consecutive cycles is carried out gradually: the mock-up is first cooled by imposing a limit of 10 °C on the thermal gradient ( $\Delta T$ ) between the core of the structure and its conservation environment. Once the  $\Delta T$  between the pool's water and the ambient temperature is below 10 °C, the basin is emptied. The pool remains empty for 3 days between two consecutive cycles allowing

macroscopic monitoring and measurement of the crack index. Then they are filled again  
 390 by imposing the same stress on the thermal gradient during the phase of rise to the  
 desired temperature level. Thereafter the duration of a cycle varies from month to month  
 depending on climatic conditions.

The mockup's conservation history is detailed in Table 5. During the first 235 days,  
 both mock-ups are conserved under water at ambient temperature. This time is  
 395 necessary to finalize the platform's construction and to set-up the temperature  
 regulation system. Afterwards, the mock-ups undergo 12 identical cycles like described  
 above (from  $t = 270$  days to approximately  $t = 770$  days). Finally, after the 13<sup>th</sup> cycle,  
 the mock-ups are conserved constantly underwater at the target temperatures for  
 approximately 400 days.

400

**Table 5:** Mock-up's conservation history

<b>Time (days)</b>	<b>Conservation condition</b>
0 - 235	Constantly immersed at ambient temperature ( $15\text{ °C} < T < 24\text{ °C}$ )
235 - 770	13 consecutive water renewal cycles, cycle duration $\approx 42$ days including a 28 days plateau at target temperature ( $38\text{ °C}$ for the ASR mock-up and $20\text{ °C}$ for the DEF mock-up)
770 - $\approx 1200$	Constantly immersed at target temperature



**Figure 11 :** Installing the DEF mock-up in its conservation pool

The basins are thermally insulated with a 10 cm layer of glass wool. The temperature regulation system consists of a pump to ensure the circulation of water, a heater and a filter (without adding chlorines). It's designed to control the temperature of each basin so as to reach a maximum temperature of 41 °C and to fully recycle the pool's water (18.7 m<sup>3</sup>) every 2 hours. The pools are instrumented with temperature sensors to constantly monitor the thermal gradient between the mock-ups core and their conservation environment during the different cycles and to guarantee the temperature uniformity in the basin (absence of stratification).

## 9. Experimental program & methods

The experimental program consists of:

- Monitoring the deformations measured by the vibrating wire extensometers placed at various heights inside the mock-ups;
- Maintaining the mock-ups' conservation environment like described above;
- Tracking the mock-ups' cracking index and mapping the surface cracking and various dates;
- Quantifying the alkalis leached during the immersion cycles. Three water samples are taken from each pool at different heights during emptying and one at each filling. These samples undergo Inductively Coupled Plasma (ICP) mass spectrometry analyzes which measures the concentrations of Sodium and Potassium in water to quantify the leaching of alkalis.
- Realizing residual expansion tests on concrete samples extracted by coring from the mock-ups. Three 11x22 cm cylinders are cored in each mock-up along the Y axis at  $z = 31$  cm (almost at  $z = 0.25H$ ). Cores extracted from the ASR mock-up are subjected to the LPC n°44 test method in which the samples mass and dimensional variations are monitored while they are stored at 38°C and RH=100% [21]. Cores extracted from the DEF mock-up are subjected to the LPC n°67 test method in which the samples mass and dimensional variations are monitored while they are stored at 20°C and immersed in water [22].

## 10. Results & Discussion

Thereafter, the main results obtained after the monitoring of the mock-ups in accordance with the experimental program are presented: the full expansion  
435 measurements provided by the embedded extensometers over a 3 years period as well as the macroscopic monitoring of cracking in the structures. A comparison between the swelling of the mock-ups and the residual swelling is carried out. Finally, feedback on the acceleration strategy is presented.

### *10.1 Dimensional monitoring of the mock-ups*

440 The automated monitoring of the mock-ups is carried out while they are maintained at constant temperature hence excluding the inter-cycle phases; therefore in isothermal conditions. The centers of the strain gauge rosettes R1, R2 and R3 are located respectively at the top ( $3H/4$ ), in the center ( $H/2$ ) and at the bottom ( $H/4$ ) of the mock-up. The extensometers contained in each rosette are named as follows:

445 ORIENTATION OF THE AXIS followed by THE ROSETTE NUMBER  
For example, "X1" identifies the extensometer oriented along the X axis and located in rosette R1.

#### *10.1.1 ASR Mock-up*

Figure 12 features the swelling in the ASR mock-up as recorded by the strain sensors.

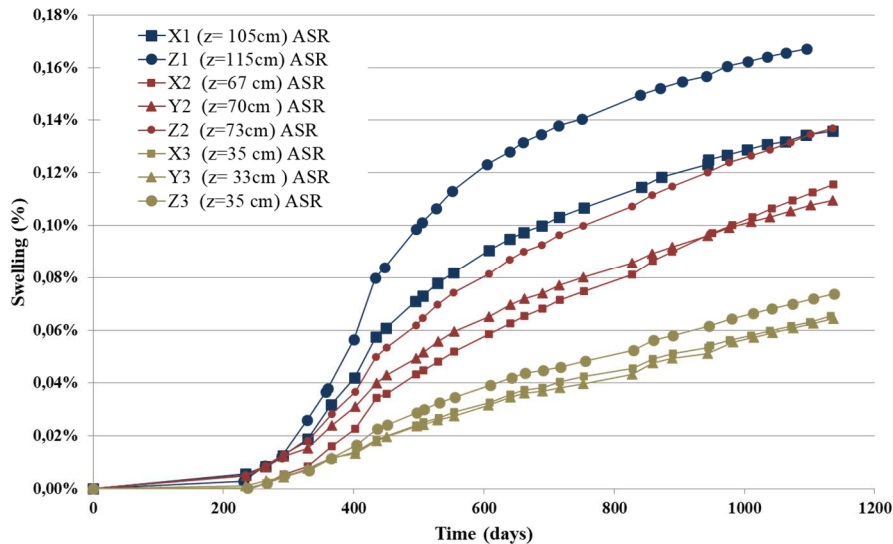


**Figure 12: Strain measurements in the ASR mock-up**

450 Until  $t=235$  days, the massive structure is conserved in water at ambient temperature. There's hardly no swelling at this stage. Once the temperature rose to  $38^{\circ}\text{C}$ , swelling in the mock-up started increasing in a similar manner to accelerated tests on laboratory specimens. Therefore, we confirm that thermo-activation is a valid method to accelerate ASR on a massive scale structure. After 700 days of follow-up, swelling in the structure

455 seems to reach the second inflection point. The maximum amplitude recorded is about  $1700\ \mu\text{m}/\text{m}$ . However this value varies according to the position of the sensor and its orientation. As a general rule, the swelling decreases as we approach the base of the structure regardless of the orientation of the sensor. Thus, a difference of approximately  $1000\ \mu\text{m}/\text{m}$  is measured between the sensors Z1( $z=115\ \text{cm}$ ) and Z3 ( $z=35\ \text{cm}$ ). A first

460 idea would be to evaluate the impact of the concrete's own weight on the deformations measured by the sensor. If we consider the Z3 sensor, the stress due to the self-weight of concrete is just  $0.024\ \text{MPa}$  at this point, which discards this hypothesis. Eventually, numerical simulations showed that this behavior is actually due to the stress generated by the restraint effect due to the friction with the metal support on which the structure

465 has been cast. The upper part of the mock-up can expand freely whereas the lower part is hindered by the support. Moreover, measures show that at lower heights the swelling in the horizontal plane parallel to the support (along X and Y) is hindered more than

the swelling measured vertically (along Z). Another approach to analyze this behavior would be to consider that the expansion, which is prevented along the directions of the metal support, is compensated by a greater expansion in the unstressed direction (Z). This effect decrease as we approach the upper part of the mock-up. As a matter of fact, the experimental campaign conducted by Larive, has shown that the mean volume swelling remains generally constant when the value of the uni-axial stress applied to the specimens remains below 10 Mpa [17]. Whereas Dunant's work [23] on concrete developing ASR and subject to uniaxial loading show that load influences the micro-crack propagation, which changes the shape of the expansion curve. The expansion is not redistributed, but the applied load forces the orientation of the micro-cracks at the micro-structural level [23]. Moreover, when tri-axial loading is considered, Liaudat's [24] work show that the volumetric ASR expansion rate is reduced as the applied volumetric compressive stress is increased. And that there seems to be an increase of the expansion rate in the less compressed direction in detriment of the expansion rates in the most compressed ones [24].

At  $t=1136$  days, the ASR mock-up's monitoring is stopped. A maximum swelling of  $1700 \mu\text{m/m}$  is recorded. However, by examining the swelling curves we deduce that even though the structure passed the second inflexion point, however the swelling didn't reach yet its full potential.

### *10.1.2 DEF Mock-up*

Figure 13 illustrates the evolution of the deformations measured in the DEF mock-up.



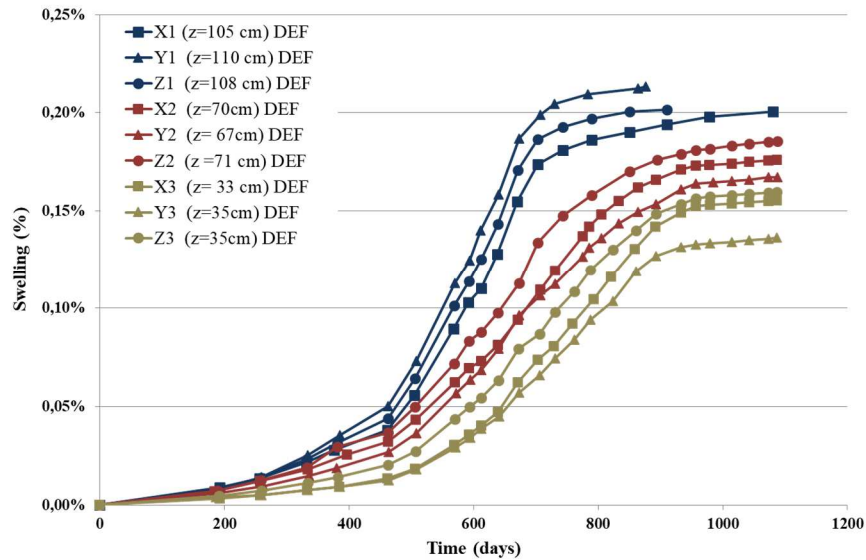


**Figure 13: Strain measurements in the DEF mock-up**

490 During the first 235 days, the DEF mock-up is conserved in the same storage conditions as the ASR mock-up. This does not seem to have a considerable impact on the reaction's kinetics for two reasons: first, because the DEF mock-up is later on stored at 20 °C which does not vary much compared to the ambient temperature. Second, because the delayed ettringite formation is characterized by a higher latent phase than the alkali-silica reaction. Swelling in the DEF mock-up accelerates at approximately  $t = 475$  days and the concrete reaches the second inflexion point around  $t = 700$  days at the R1 level and around  $t = 900$  days at the R2 and R3 levels. Knowing that the extensometer's precision is guaranteed by the manufacturer up to 2000  $\mu\text{m}/\text{m}$ , we suspect that the R1 measurements after  $t = 700$  days are not accurate because the maximum capacity of the strain gage is reached. We observe a similar mechanical behavior as the ASR mock-up: the swelling decreases as we approach the base of the structure regardless of the orientation of the sensor. Thus, a difference of approximately 500  $\mu\text{m}/\text{m}$  is measured between the sensors Z1( $z = 108$  cm) and Z3 ( $z = 35$  cm) at  $t = 805$  days which further corroborates the previous hypothesis that the upper part of the mock-up can expand freely whereas the lower part is hindered by adherence with the metallic support.

495

500

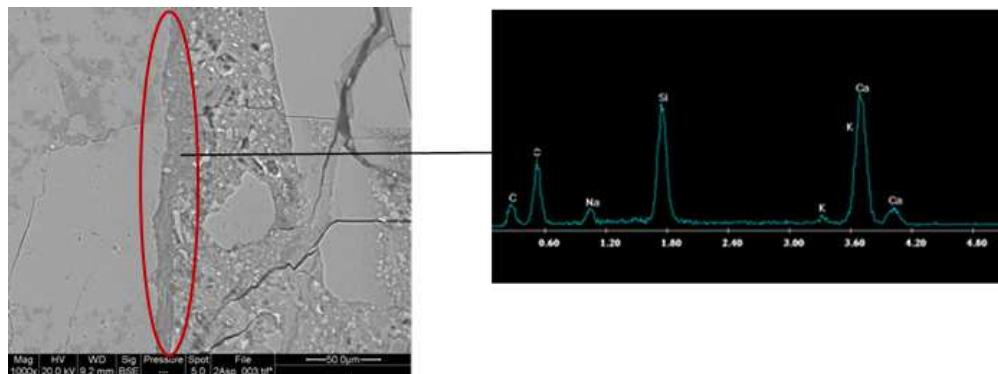
505

At t=1080 days, the DEF mock-up's monitoring is stopped. A maximum swelling of 2130  $\mu\text{m}/\text{m}$  is recorded (beyond which the stain sensor broke). By examining the swelling curves we deduce that the swelling reached the stabilization phase.

## 510 10.2 Investigating the origin of the swellings using Scanning Electron Microscopy (SEM)

To determine the cause of the expansion, polished concrete samples taken from both mock-ups are examined by scanning electron-microscopy (SEM) with energy-dispersive X-ray spectroscopy (EDXS).

515 The examination of specimen extracted at t = 300 days of age from the ASR mock-up (Figure 14) revealed the presence of alkali-reaction gel at the paste-aggregate interface. This is confirmed by the associated elemental spectrum which identifies the following elements: Silica, Calcium, Potassium, Sodium and Oxygen.

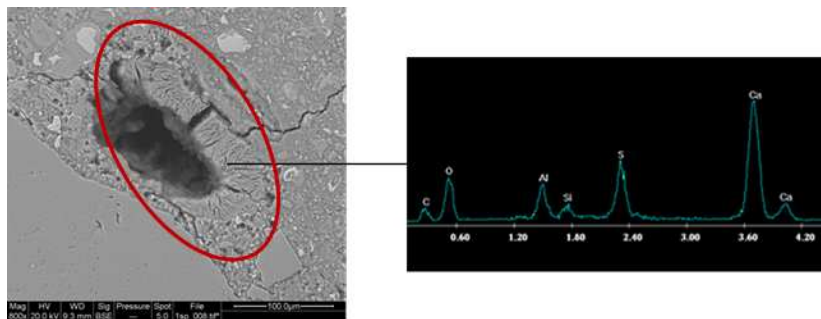


520 **Figure 14: SEM image of a polished concrete sample extracted from the ASR mock-up at t = 300 days of age and associated elemental spectrum**

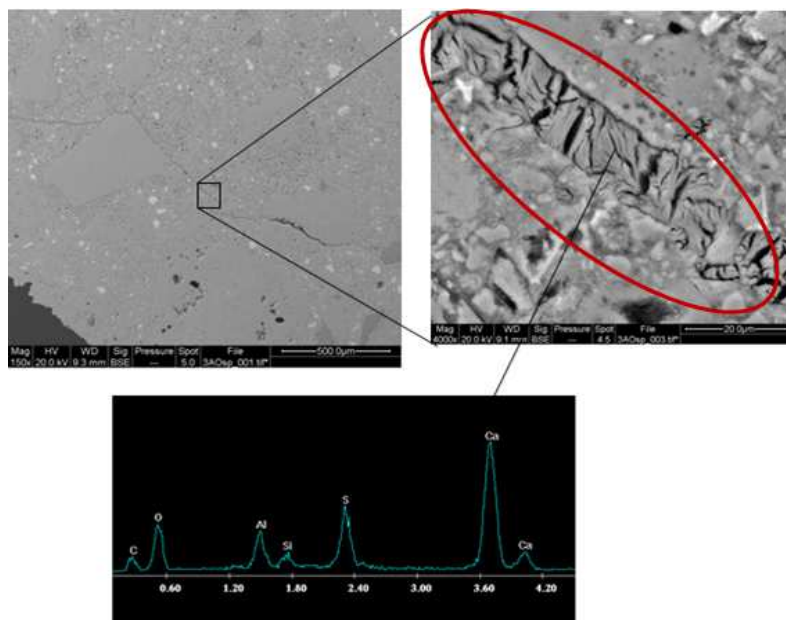
At t = 300 days, the ASR mock-up is in the swelling acceleration phase (see Figure 12). Therefore, microscopic observations confirm that the origin of the swelling measured is due to the formation of the alkali-silica gel and show also that the concrete exhibits a good cohesion within the cement matrix and at the aggregate/cement paste interfaces.

525 Figure 15 shows scanning electron micrographs of polished concrete samples extracted at t = 261 days of age from the DEF mock-up. The images show ettringite filling pores and cracks in the cement paste. This is confirmed by the associated elemental spectrum which identifies the following elements: Calcium, Sulfate, Aluminum and Oxygen. Figure 15b shows a microcrack propagating through the

530 cementitious matrix and crosses the interface between an aggregate and the surrounding  
paste. The opening of this microcrack is approximately 10  $\mu\text{m}$  and it is filled with  
needle-shaped ettringite more or less oriented perpendicular to the crack and has a  
compressed appearance. At this stage (see figure 13 for  $t = 261$  days), the DEF mock-up  
is still in the linear latent phase. Nonetheless, the SEM observations depict the  
535 presence of ettringite both in the cement paste and at the aggregate/paste interfaces  
which confirms that the cause of the expansion measured in the DEF mock-up is indeed  
the delayed ettringite.



(a)



(b)

**Figure 15 : SEM images of polished concrete samples extracted from the DEF mock-up at t = 261 days of age and associated elemental spectrums**

### 10.3 Macroscopic monitoring of the mock-ups

Macroscopic monitoring of the mock-ups permits to correlate the internal swelling  
 540 of the structure with the evolution of visible cracking. The use of the LPC No.47 test  
 method allows characterizing the structure's state of damage at a given time by referring  
 to an established classification based on the cracking index's value (negligible, low,  
 moderate, high, very high, considerable) but also to monitor the cracks' evolution over  
 time [18]. Figures 16 and 17 feature the evolution of the cracking index in the ASR and  
 545 in the DEF mock-ups respectively.

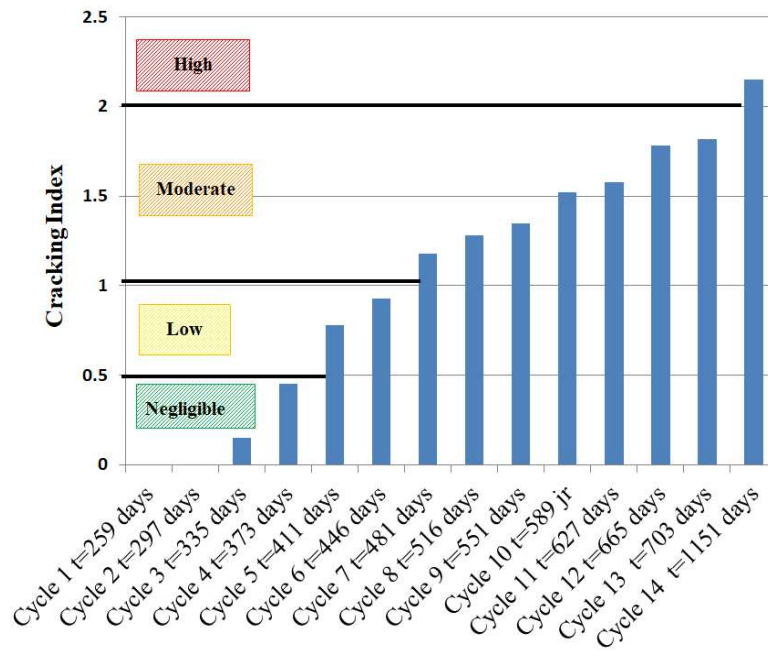


**Figure 16: Evolution of the cracking index in the ASR mock-up (mm/m<sup>2</sup>)**

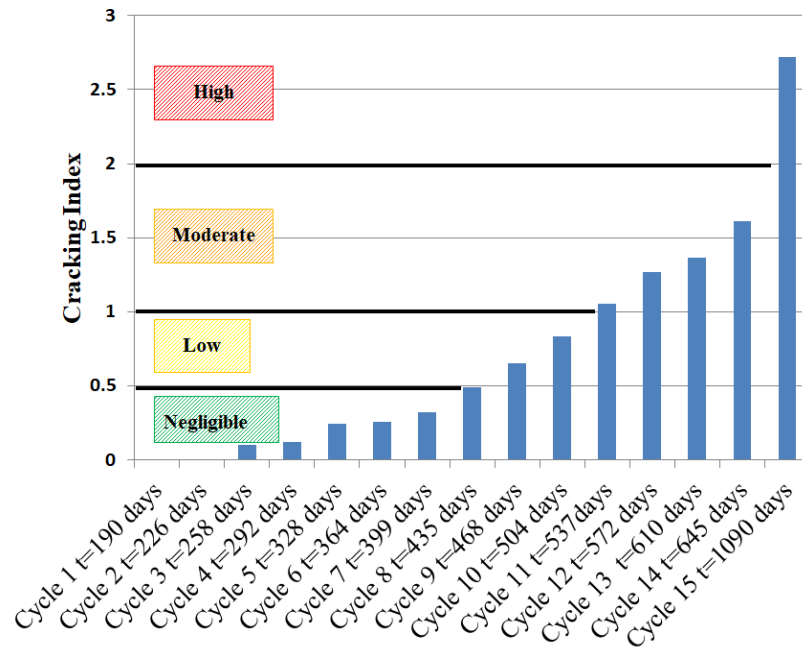


**Figure 17: Evolution of the cracking index in the DEF mock-up (mm/m<sup>2</sup>)**

According to the classification proposed by this test method, currently the ASR and the DEF mock-ups are subject to a “high” cracking and are considered damaged by the internal swelling reactions. Both mock-ups maintained a “negligible” and a “low” cracking during the first cycles which correlates well with the internal swelling measurements. Matter of fact, the DEF mock-up is characterized by a long latent phase (up to t = 450 days approximately) which is reflected by a negligible cracking up to cycle 8 (t = 435 days).

However, a visual inspection of these structures reveals that the cracking is not uniform on their envelope. The cracking index, as a parameter, expresses an average crack opening over one square meter but does not give information on the orientation and distribution of the cracks. Subsequently, in order to enrich the information provided by this test method and to provide a more global vision of the damage at the structure level, a crack mapping is carried out. The coordinates of the crack points were carefully noted as well as the opening of the corresponding cracks. The cracks are then classified into five categories according to their width. Figures 18 to 21 illustrate the maps obtained at chosen time stamps as well as photographs of the deteriorated mock-ups.

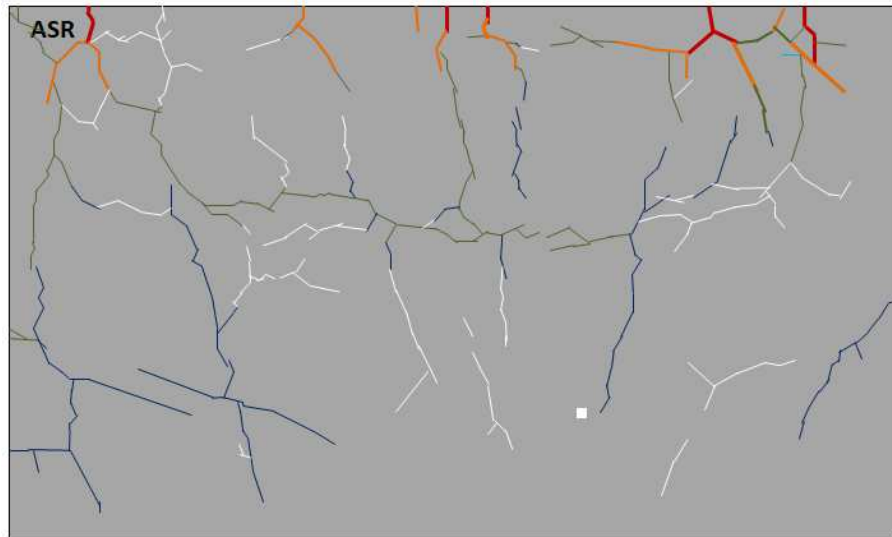


**Figure 18 : Cracks mapping of the ASR mock-up at t = 703 days**



**Figure 19: Photo of the ASR mock-up at t = 703 days**

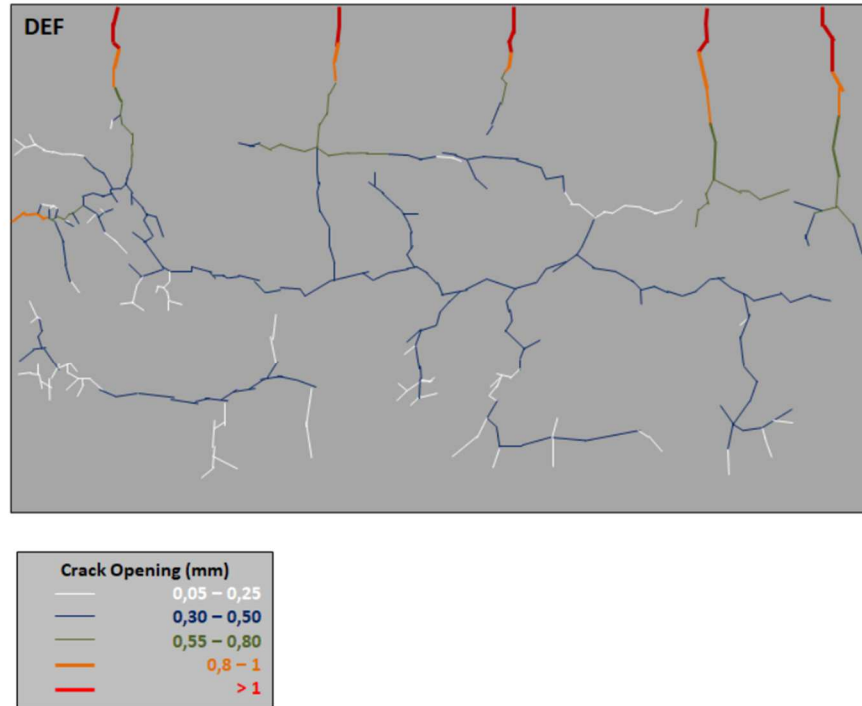


Figure 20 : Cracks mapping of the DEF mock-up at t = 1195 days



Figure 21: Photo of the DEF mock-up at t = 1195 days

We observe the presence of a main longitudinal crack around mid-height and vertical cracks at the top of both mock-ups. The opening of the vertical cracks is greater than 1 mm in the upper part and decreases as we approach the lower part.

565 From a mechanical point of view, the vertical cracks on the upper part of the mock-ups correlate directly with the differential deformations measured along the X axis at the rosette R1 level in comparison with the rosette R3 level. These differential deformations can be explained by the presence of the metal support in the lower part of the structure. In his work on reinforced and non-reinforced beams affected with DEF, Martin [25] 570 shows that the presence of reinforcements reduces longitudinal deformations. In addition to that, the longitudinal cracks are parallel to the metal support in both mock-ups. This seems to confirm the hypothesis of anisotropy induced by the presence of steel. In fact, numerous studies show that the crack orientation of a concrete affected by an internal swelling reaction is a function of the direction of reinforcement or of pre- 575 stressing. The works of [25] and [26] show that the swellings induced by DEF are isotropic under free swelling conditions but become anisotropic as soon as a loading is applied. As for ASR, the works of [17] [27] [28] and [29] join the hypothesis that an external loading (even passive) generates a redistribution of swellings in the least compressed directions. Moreover, [17] and [29] highlight that the direction of concrete 580 casting can also induce anisotropy related the development of the alkali reaction. The direction of the fresh concrete flow influences the orientation of the aggregates as well as the distribution of water around these aggregates, which impacts the swellings and the cracking in the event of an alkali reaction. Results show that cracks often appear perpendicular to the direction of the concrete casting flow. This phenomenon could 585 explain as well the important opening of the main longitudinal crack in both structures. Furthermore, the manufacturing methodology and in particular the care taken to avoid cold joints guarantee the homogeneity of the block and allow to dismiss the hypothesis that the horizontal cracks are due to the successive concrete batches. Mechanical tests on concrete samples taken from two successive mixes further confirm this theory.

590 All cracks are filled with white precipitation on the surface of both mock-ups. DRX analyzes show that it is calcite due to ionic leaching during the immersion cycles. It is noted that the volume of the precipitate increases with the opening of the cracks. This product is then scrubbed out in order to allow the measurement of the crack openings.



595 Figures 22-a to 22-d show cracks which cross several planes of the mock-ups (XZ, YZ and XY planes according to the convention established previously). This confirms that the damage affects the structure as a whole.



**Figure 22 : (a) DEF mock-up at t = 537 days (b) DEF mock-up at t = 537 days  
(c) ASR mock-up at t = 512 days (d) ASR mock-up at t = 516 days**

#### *10.4 Residual swelling of the mock-ups*

The coring of the structures took place on t = 206 days of age for the ASR mock-up and t = 161 days for the DEF mock-ups. Figure 12 and figure 13 show negligible swelling at this time in both mock-ups hence the residual swelling obtained with these  
600

cores represents the maximum swelling these structures could reach. The use of core samples as opposed to molded samples makes it possible to obtain a homogeneous distribution of the aggregates in the test samples according to [30] and thus to avoid skin effects. However, it should be kept in mind that the coring induces micro-cracks due to the high speed action of the drill which can affect the transfer properties in the test samples. Residual expansion tests are tools frequently used in the assessment of structures affected by internal swelling reactions. In particular, they make it possible to assess whether the disorders due to an internal swelling reaction are likely to worsen in the future or whether they have already stabilized. Furthermore, these tests constitute one of the main input data for certain numerical simulation methods, in particular because they allow calibrating the chemical progress of the reactions [31].

Figure 23 shows the swelling in the cores subjected to the LPC N°44 test method (CR\_ASR\_38\_100HR) in comparison to that of the ASR mock-up.

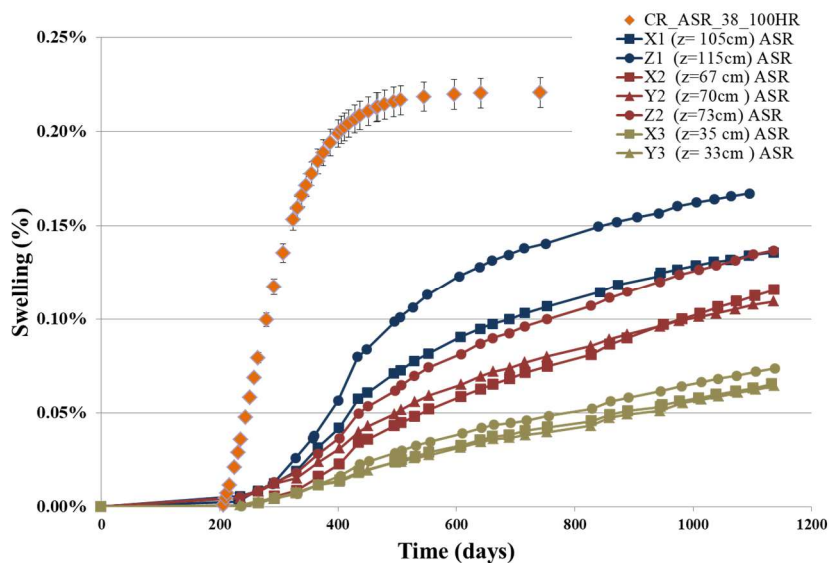


**Figure 23: Residual swelling in the cores extracted from the ASR mock-up**

The ASR cores yield a residual swelling of 0.22% while the maximum strain measured in the upper part of the mock-up is 0.17%. They present no latency time and swelling initiated in those samples as soon as they are conserved at 38°C. By comparing their behavior with that of the structure, we notice that even though the swelling in both sample types is thermo-activated, however the swelling amplitude and kinetics differs greatly from one to another: first, the cores yield a residual swelling of 0.22% whereas

620 the maximum strain measured in the upper part of the mock-up is 0.17% (and expected to stabilize at around 0.185%). Second, the swelling in the cores stabilizes in about 400 days whereas the dimensional variations in the ASR mock-up didn't stabilize even after 900 days of conservation at 38°C.

Figure 24 compares the strain evolution in the DEF mock-up with the dimensional monitoring of the corresponding cores subjected to the LPC N°67 test method (CR\_DEF\_20\_Imm).

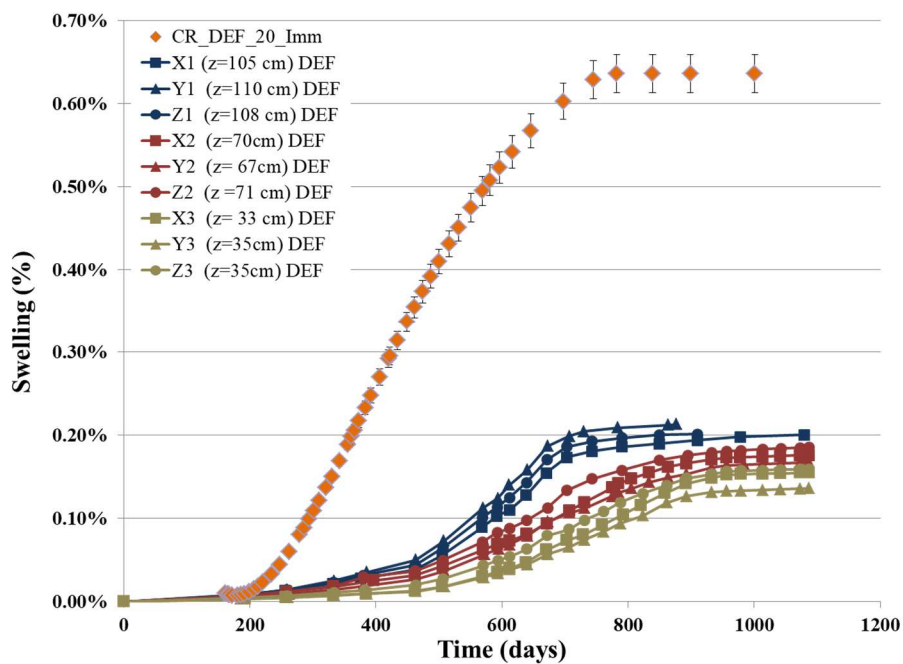


**Figure 24: Residual swelling in the cores extracted from the DEF mock-up**

The dimensional monitoring of the DEF cores reveal similar trends as those observed earlier in terms of final amplitudes and kinetics. They yield a residual swelling of 0.65%, almost three times higher than the maximum strain measured in the upper part of the mock-up which is 0.22%. In terms of kinetics, the swelling in the DEF cores stabilize approximately 500 days earlier than the mock-up's.

The concrete in the lower part of the mock-ups is subject to confinement constraints due to the presence of the metal support and to the concrete weight. The comparison between the coring samples and the lower part of the structures therefore leads to comparing concrete swellings which are in distinct states of stresses: the cores are

almost completely free to swell whereas the mock-ups are subjected to passive stresses. However, by limiting the comparison to the upper (free) part of the mockups, the measured gap implies the presence of a scale effect due to the difference in size between these two types of samples. Moreover, the size of the cores in comparison to that of the massive structures renders diffusive phenomena faster given they both have the same chemical potential and assuming they are both conserved in the same hydric conditions. Among these phenomena, alkali leaching occur faster in the coring samples in comparison to the mock-up in the DEF case for instance. This explains the difference in the reactional kinetics. It should also be noted that the additional micro-cracking induced by coring would allow new precipitates formed during the expansion test to fill these voids before swelling occurs, thereby reducing the measured residual expansion.

### *10.5 Discussion on the ASR acceleration strategy*

The approach proposed to develop ASR at the level of a massive structure involves two main parameters which influence the kinetics of this pathology:

- o The choice of reactive aggregates (type of reactive silica) and the granular composition.

- o The conditions of water and thermal conservation of the mock-up.

There is no information available to assess the effect of the first parameter since only one concrete composition is used in this study. However, the macroscopic monitoring as well as the strain measurements in the mock-up highlight the impact of the storage temperature on the kinetics of the alkali-aggregate reaction and attest that the swelling touches the whole structure and is not localized. This confirms that such a process is valid for accelerating ASR in massive structures. However, the Institute of Structural Engineers [32] recommends tests at the annual average temperature of the structure studied, arguing that expansions at 38 ° C, although faster, do not always reach values as high as testing at colder temperatures and alter the gel's chemical composition. However, in our case the use of a temperature of 38°C is necessary to obtain expansion results within the project's time table.

Furthermore, an eventual criticism of the proposed approach could be that the water cycles induce alkali leaching which is unfavorable for the development of ASR. Figure

25 illustrates the amounts of alkalis leached at each cycle and Figure 26 illustrates the cumulative amounts of leached alkalis.

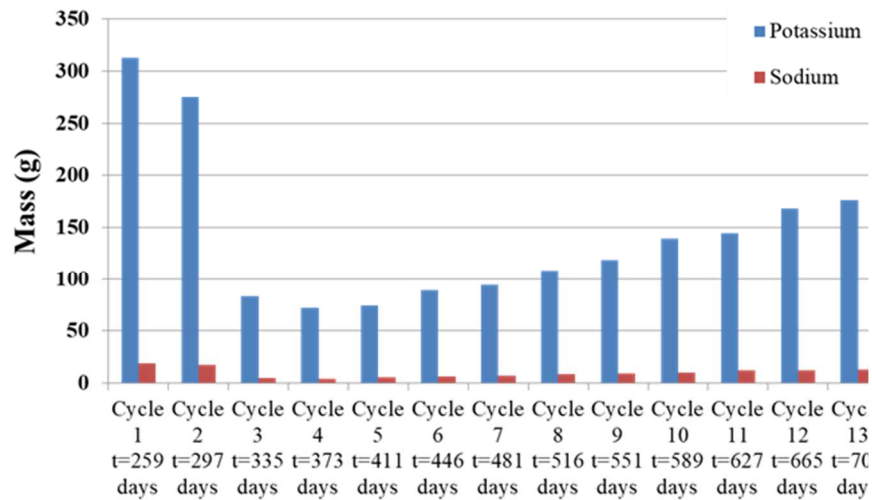


**Figure 25 : Mass quantities of alkalis leached at each cycle – ASR mock-up (the mass is the total mass of sodium and potassium present in the water used for immersion)**

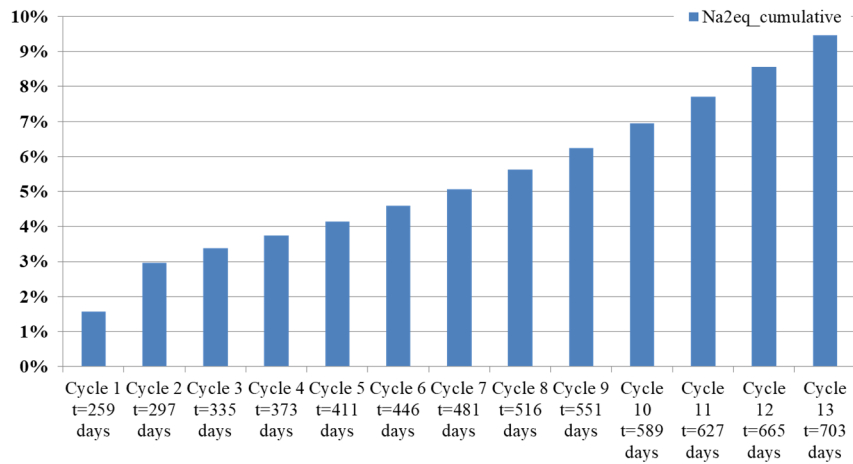


**Figure 26 : Cumulative amounts of alkalis leached - ASR mock-up (the percentages apply to the total alkali content of the concrete mix)**

We deduce that the cumulative amount of equivalent alkalis leached is 9.5% of the initial amount contained in the mock-up which is not negligible. We assume that this amount is larger than the quantity of alkalis leached from the coring samples knowing

that they are conserved at 100% relative humidity and not immersed like the ASR mock-up. This result explains the difference in the swelling amplitude between both sample types and suggests that the pathology is more developed at the core than at the skin of the structure. However, the fact that the mock-up is submerged provides a significant amount of water which is also an essential reactant for the development of the reaction. In practice, the conservation of the structure at 100% relative humidity in order to limit the leaching of alkalis is very difficult to set up given the size of the test body. If the pools are not emptied regularly, then macroscopic monitoring of the mock-ups wouldn't be possible. In addition, the closed-cycle pumping of the water, assured by the regulation system, guarantees a uniform temperature distribution in the pool. A solution to prevent from alkalis leaching would be to add alkalis to the pool's water so as to eliminate the concentration gradient. In the case of this study, this idea is not retained for safety and environmental reasons given the important volume of water in question (18.7 m<sup>3</sup> per cycle). In conclusion, the results obtained are considered satisfactory and validate the proposed approach. However, a possibility of improvement would be to reduce the leaching of alkalis induced by water change cycles.

### *10.6 Discussion on the DEF acceleration strategy*

Monitoring the expansion in the DEF mock-up reveals a latent phase of 500 to 600 days. This duration is greater than the latent phases usually found after applying accelerated test protocols on laboratory samples, such as in the LPC N°66 performance test [4] [33]. However, it remains far below the latent phases commonly observed in massive structures in real life (around 5 to 15 years). The strategy proposed to accelerate DEF in the massive mock-up involves two parameters: first, the thermal profile at a young age which controls the amount of ettringite dissolved at a young age; second, the water change cycles which leads to alkali leaching.

In order to assess the efficiency of the proposed strategy, we will first compare the measured early-age thermal profile of the DEF mock-up with that of a hypothetical mock-up that did not undergo a heat treatment at the early age. The thermal profile of the hypothetical structure is determined via a numerical simulation. It is assumed that the concrete temperature is equal to the ambient temperature on the day of casting, ie 25°C, and that the hypothetical structure is cast in an ordinary wooden formwork. These

results are then compared to the thermal profile actually measured within the DEF mock-up as featured in Figure 27.

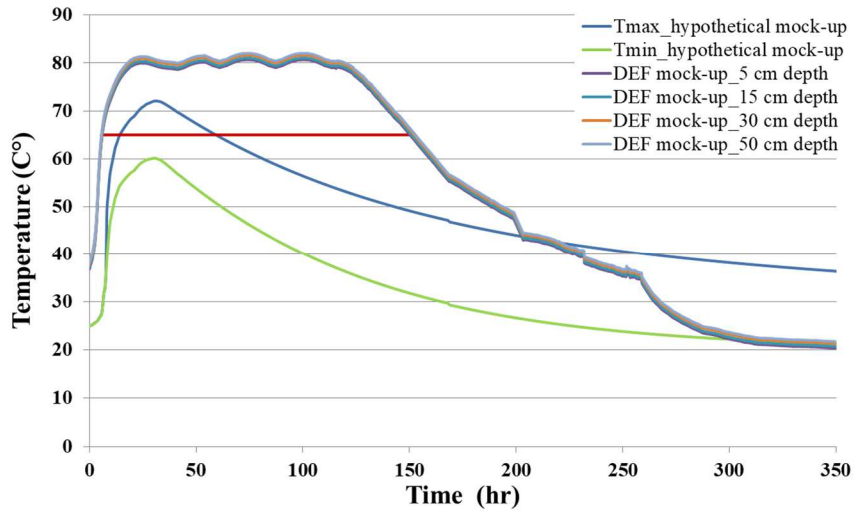


**Figure 27: Comparison between the thermal profiles of the DEF mock-up and the hypothetical mock-up**

705 Figure 28 compares the temperature field measured in the DEF mock-up with the temperature field simulated for the hypothetical mock-up at the maximum temperature instant.

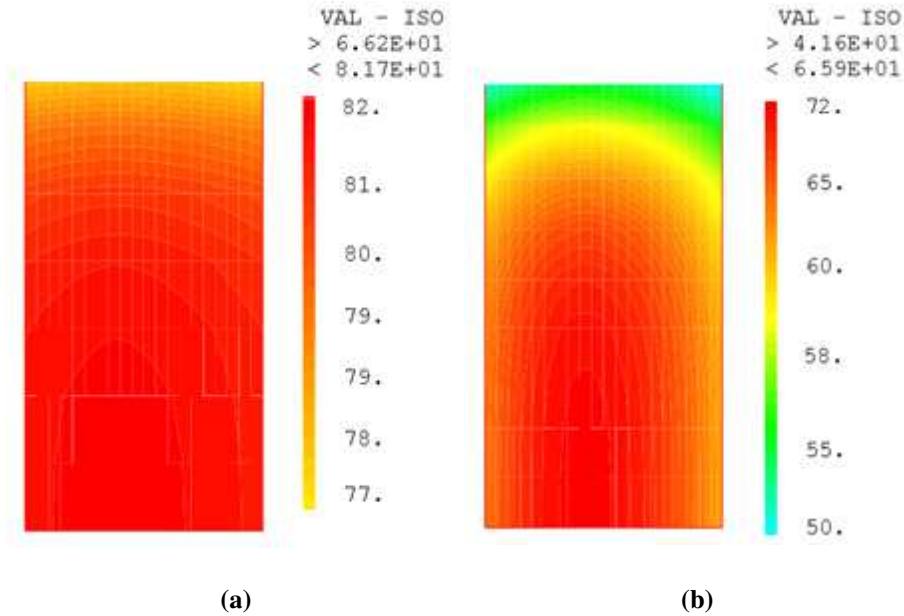
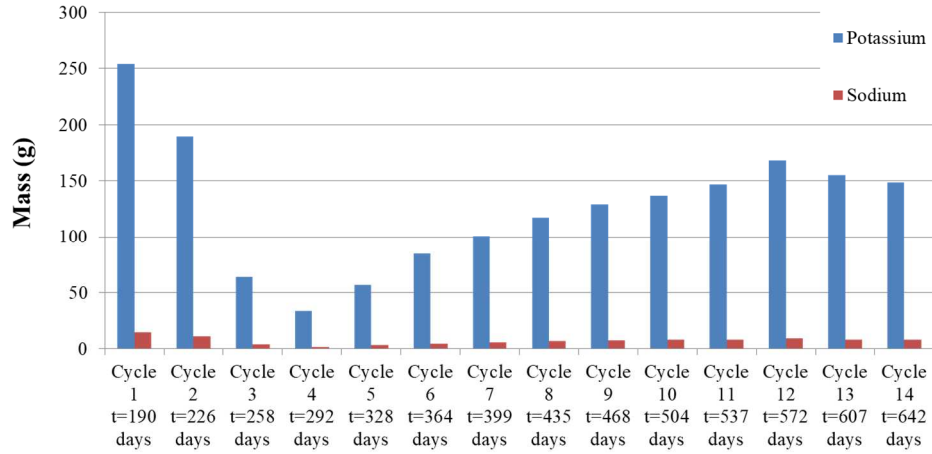


**Figure 28 : Temperature field as measured in the DEF mock-up (a) and in the hypothetical mock-up (b) at the maximum temperature instant**

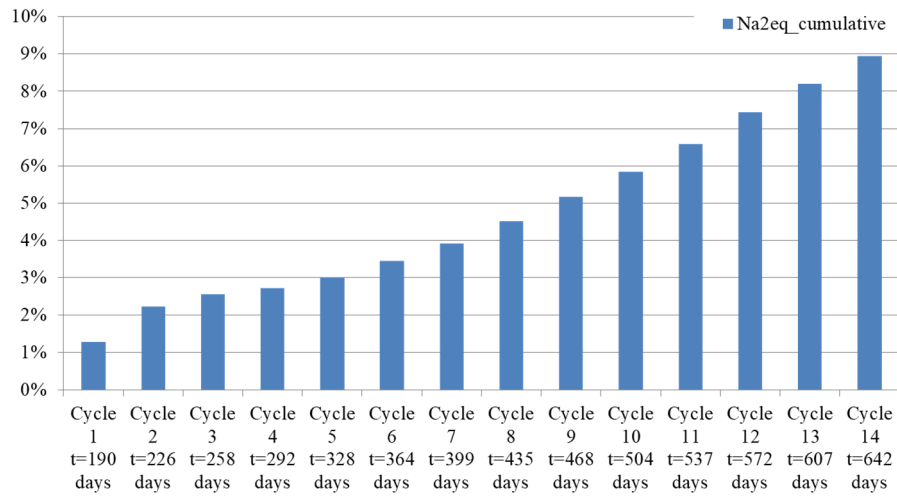
Two major differences are revealed. First, the effective thermal energy (EU) in the case of the hypothetical mock-up is approximately 175 °C.hr, or about 11% of the energy communicated to the DEF mock-up by the early-age temperature regulation system installed. This factor has a significant impact on the latent period and the final expansion. According to the empirical modeling established by [10], this induces a final swelling in the hypothetical mock-up of about 15% of that measured in the DEF mock-up and a longer latent phase. It should also be noted that the maximum temperature reached by the theoretical structure is 72°C while the DEF mock-up has actually reached 82°C. According to the thermodynamic model established by [8], 10 times more ettringite is dissolved at 82 °C than at 72 °C (and 10,000 times more at 85°C than at 20°C). We deduce that the proposed early-age strategy succeeded in initiating and boosting the pathology by maximizing the amount of ettringite dissolved at the early-age thanks to the controlled thermal profile. However, an improvement could be made as to the representativeness of the thermal history for future mock-ups. Second, this simulation highlights a non-homogeneous temperature field (with a  $T_{\max} > 65^{\circ}\text{C}$  at the core and  $T_{\max} < 65^{\circ}\text{C}$  near the edges) in the theoretical mock-up which leads to a non-homogeneous field of ettringite formation. This phenomenon combined with the fact that the environmental conditions and the alkalis leaching act mainly on the surface is among the factors causing the long latency periods before the manifestation of DEF in massive structures. Conversely, the temperature field is rather homogeneous in the DEF mock-up and a homogeneous field of ettringite formation is ensured similarly to laboratory samples.

Figure 29 illustrates the amounts of alkalis leached at each cycle and Figure 30 illustrates the cumulative amounts of leached alkalis from the DEF mock-up.





**Figure 29 : Mass quantities of alkalis leached at each cycle – DEF mock-up (the mass is the total mass of sodium and potassium present in the water used for immersion)**



**Figure 30 : Cumulative amounts of alkalis leached – DEF mock-up (the percentages apply to the total alkali content of the concrete mix)**

The high quantity of alkalis leached in the first cycle is certainly due to the fact that the mock-up is kept in water for 190 days before the first emptying. This quantity decreases during the 3 following cycles then gradually increases again until cycle 12. This reduction is due to the leaching of the alkalis which are found concrete skin. However, the increase in the quantities of potassium and sodium leached from cycle 4 is probably due to the development of cracking in the mock-up which increases the interaction

740 surface between water and concrete. Moreover, the fact that leaching mainly affects the  $K^+$  ions is due to the composition of the cement which contains 1.5% by mass of  $K_2O$  and only 0.07% of  $Na_2O$ , and it is also due to the fact that the ionic mobility of potassium is greater than that of sodium ( $\mu_{Na^+} = 52.10 \cdot 10^{-9} \text{ m}^2 \cdot \text{V}^{-1} \cdot \text{s}^{-1} < \mu_{K^+} = 76.21 \cdot 10^{-9} \text{ m}^2 \cdot \text{V}^{-1} \cdot \text{s}^{-1}$  at  $25^\circ\text{C}$ ). Figure 31 shows the evolution of the quantity of equivalent alkalis leached as a function of the cracking index of the DEF mock-up starting from cycle 4. (The value of the cracking index is zero in prior cycles).

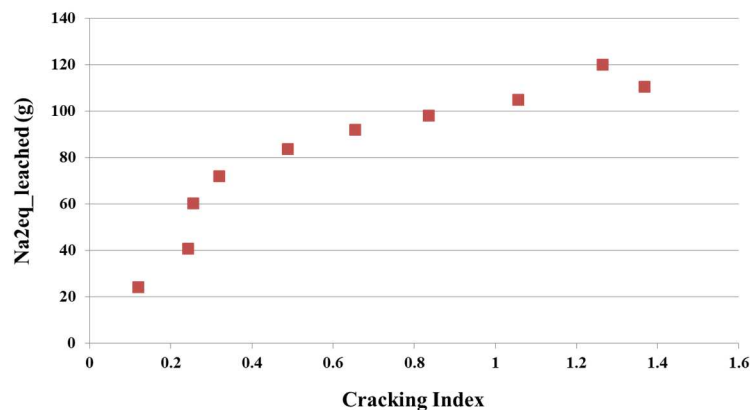


**Figure 31 : Evolution of the quantity of equivalent alkalis leached as a function of the cracking index of the DEF mock-up**

745 This graph shows that from cycle 4, the quantity of leached alkali increases in proportion to the cracking index, which confirms the hypothesis previously stated. As a matter of fact, alkalis' leaching lowers the pH of the interstitial solution of the concrete. This accelerates the desorption of sulfates, consequently increasing the quantity of precipitated ettringite [7] and amplifying the damage of the concrete.

750 Increased swelling leads to a larger crack opening and therefore, an even greater amount of alkalis leached in the next cycle and so on. These results confirm the simulation approach of [8] that links the kinetics of ettringite precipitation in a concrete specimen stored in water to the rate of alkalis' leached which shows the importance of this parameter in the kinetics of the delayed ettringite formation. Finally, these results

755 validate the proposed DEF acceleration strategy and further corroborate the choice of ensuring a homogeneous thermal profile in the mock-up while imposing water change cycles during the conservation phase. However, it would have been interesting to test the influence of a storage temperature of  $38^\circ\text{C}$  instead of  $20^\circ\text{C}$  on the development of DEF at the scale of a massive structure.

760 **11. Conclusions**

Internal swelling reactions are complex phenomena that involve the coupling of several chemical, thermo-dynamic, hydric and mechanical aspects. The difficulty of understanding the mechanism leading to the appearance of expansions and the scale effects on the kinetics of these pathologies are still subjects of debate in the scientific community. In this paper, experimental approaches to accelerate alkali-silica reactions and delayed ettringite formation on the scale of a massive structure has been developed to allow better observation and understanding of swelling reactions at such a scale. Two representative massive concrete structures (2.4 x 1.4 x 1 m<sup>3</sup>) were realized under controlled and optimized conditions for the development of both internal swelling reactions. The evolutions of the pathologies in the massive structures are monitored both internally and externally. The respective deformations and cracking were tracked for over 3 years as well as the thermal, hydric and chemical environments of the mock-ups.

The strategy employed to accelerate those pathologies at such a scale consists of optimizing the main parameters influencing the kinetics of the reactions (reactants quantities, temperature and homogeneity) while avoiding artificial mechanical damage of the test samples. Results show that expansions in massive structures vary greatly from analogous laboratory samples. Boundary conditions and confinement effects could hinder swelling along certain directions thus compensated by a higher expansion along unstressed directions which leads to an anisotropic behavior in the material and impacts the cracking orientation.

Residual swelling tests reveal the chemical potential of the internal swelling reactions and define an upper strain limit for the structure. The size of the cores in comparison to that of the massive structures renders diffusive phenomena faster given they both have the same chemical potential. The comparison reveals a scale effect on the reactional kinetics and on the swelling amplitude.

The feedback on the acceleration strategy shows that in the case of the DEF mock-up, the alkalis' leaching due the renewal of the conservation water triggers the precipitation of ettringite. The increased swelling leads to larger cracks width and therefore, an even greater amount of alkalis leached in the following cycle which creates an amplifying effect. Whereas in the case of the ASR mock-up, alkali leaching is

unfavorable for the development of the pathology because it reduces the quantity of one of the reactants. Nevertheless, the obtained results allow validating the proposed approach.

795 It ought to be mentioned that similar results were obtained in a parallel study investigating the concomitance of ASR and DEF and that will be published later.

## References

- 800 [1] Chénier J.-O., Komljenovic D., Gocevski V., Picard S., Chrétien G. (2012). An Approach Regarding Aging Management Program for Concrete Containment Structure at the Gentilly-2 Nuclear Power Plant. 33rd Annual Conference of the Canadian Nuclear Society. <https://doi.org/10.13140/2.1.2516.8645>
- 805 [2] Scrivener K.L., Damidot D., Famy C. (1999). Possible mechanisms of expansion of concrete exposed to elevated temperatures during curing (also known as DEF) and implications for avoidance of field problems, *Cement, Concrete and Aggregates*, 21(1), 93-101.
- 810 [3] Ulm F.-J., Coussy O., Li K., Larive C. (2000). Thermo-Chemo-Mechanis of ASR Expansion in Concrete Structures. *Journal of Engineering Mechanics-ASCE*. [https://doi.org/10.1061/\(ASCE\)0733-9399\(2000\)126:3\(233\)](https://doi.org/10.1061/(ASCE)0733-9399(2000)126:3(233)).
- [4] Pavoine A., Divet L., Fenouillet S. (2006). A concrete performance test for delayed ettringite formation: Part I optimisation. *Cement and Concrete Research*. 36.
- 815 [5] Petrov N., Tagnit-Hamou A. (2003). Is microcracking really a precursor to DEF and consequent expansion?, *ACI Materials Journal*, 101(6), 442-447.
- [6] Guédon-Dubied J.S., Cadoret G., Durieux V., Martineau F., Fasseu P., Overbecke V. (2000). Study on Tournai limestone in Antoing Cimescaut Quarry. 11th International Conference on Alkali-Aggregate Reaction in Concrete. 335-344.
- 820 [7] Sellier A., Multon S. (2018). Chemical modelling of Delayed Ettringite Formation for assessment of affected concrete structures. *Cement and Concrete Research*. Vol. 108. pp. 72-86.

- 825 [8] Salgues M., Sellier A., Multon S., Bourdarot A., Grimal E. (2014). DEF modelling based on thermodynamic equilibria and ionic transfers for structural analysis. *European Journal of Environmental and Civil Engineering*. 18 (4). pp. 377–402.
- [9] Ulm F.-J., Coussy O. (1995). Modeling of thermo-chemo-mechanical couplings of concrete at early ages. *Journal of engineering mechanics*. Vol. 121(7). pp. 785–794.
- 830 [10] Kchakech B., Martin R.-P., Metallssi O., Toutlemonde F. (2015). Experimental study of the influence of the temperature and duration of heat treatments at early age on the risk of concrete expansion associated with Delayed Ettringite Formation. <https://doi.org/10.1061/9780784479346.055>.
- 835 [11] Baghdadi N., Seignol J.-F., Martin R.-P., Renaud J.-C., Toutlemonde F. (2008). Effect of early age thermal history on the expansion due to delayed ettringite formation: experimental study and model calibration, *Advances in Geomaterials and Structures*.
- [12] Famy C., Scrivener K.-L., Atkinson A., Brough A.-R. (2002). Influence of the storage conditions on the dimensional changes of heat-cured mortars. *Cement and Concrete Research*, Vol. 31, n° 5, p. 795-803
- 840 [13] Scherer G.W. (2008). Factors affecting crystallisation pressure, *International RILEM TC 186-ISA workshop on Internal Sulfate Attack and Delayed Ettringite Formation*, Villars, Switzerland, 139-154.
- 845 [14] Al-Shamaa M., Lavaud S., Divet L., Colliat J.-B., Nahas G., Torrenti J.-M. (2016). Influence of limestone filler and of the size of the aggregates on DEF. *Cement and Concrete Composites*, Elsevier, 2016. pp. 175-180.
- [15] Poyet S., Sellier A., Capra B., Foray G., Torrenti J.-M., Cognon H., Bourdarot E. (2007). Chemical modelling of Alkali Silica reaction: Influence of the reactive aggregate size distribution. *Mater Struct* 40, 229.
- 850 <https://doi.org/10.1617/s11527-006-9139-3>
- [16] Monnin Y., Dégrugilliers P., Bulteel D., Garcia-Diaz E. (2006). Petrography study of two siliceous limestones submitted to alkali-silica reaction. *Cement and Concrete Research*. 36. 1460-1466.

- 855 [17] Larive C. (1997) Apports combinés de l'expérimentation et de la modélisation  
à la compréhension de l'alcali-réaction et de ses effets mécaniques. PhD thesis,  
Ecole Nationale des Ponts et Chaussées.
- [18] Fasseu P., Michel M. (1997). Détermination de l'indice de fissuration d'un  
parement de béton - Méthode d'essai LPC N47. Laboratoire Central des Ponts  
et Chaussées.
- 860 [19] Briffaut M., Nahas G., Benboudjema F., Torrenti J-M. (2010) Numerical  
simulations of the QAB and Langavant semi-adiabatic tests: Analysis and  
comparison with an experimental campaign. Bulletin des Laboratoires des  
Ponts et Chaussées.
- [20] Honório T., Bary B., Benboudjema F. (2015). Factors affecting the thermo-  
chemo-mechanical behaviour of massive concrete structures at early-age.  
865 *Materials and Structures*, Springer Verlag. Vol. 49 (8). pp. 3055 - 3073.
- [21] Fasseu P. (1997). Alcali-réaction du béton : Essai d'expansion résiduelle sur  
béton durci. Méthode d'essai LPC n° 44. *Techniques et méthodes des  
laboratoires des ponts et chaussées*.
- 870 [22] Méthodes d'essai des lpc n°67. (2009). Réaction sulfatique interne. Essai  
d'expansion résiduelle sur carotte de béton extraite de l'ouvrage. *Techniques  
et méthodes des laboratoires des ponts et chaussées LPC*.
- [23] Dunant, C. F., & Scrivener, K. L. (2012). Effects of uniaxial stress on alkali-  
silica reaction induced expansion of concrete. *Cement and concrete research*,  
875 42(3), 567-576.
- [24] Liaudat J, et al. "ASR expansions in concrete under triaxial confinement."  
*Cement and Concrete Composites* 86 (2018): 160-170.
- [25] Martin R.-P., Renaud J.-C., Multon S., Toutlemonde F. (2012). Structural  
behavior of plain and reinforced concrete beams affected by combined AAR  
880 and DE. 14th International conference on alkali aggregate reaction ICAAR14,  
May 2012, France.
- [26] Bouzabata H., Multon S., Sellier A., Houari H. (2012). Effects of restraint on  
expansion due to delayed ettringite formation. *Cement and Concrete Research*,  
42. pp. 1024–1031.

- 885 [27] Multon S., Toutlemonde F. (2006). Effect of applied stresses on alkali-silica  
reaction-induced expansions. *Cement and Concrete Research*, 36. pp. 912–  
920.
- [28] Hobbs D.W. (1981). The alkali-silica reaction - a model for predicting  
expansion in mortar. *Magazine of Concrete Research*. 33. pp. 208–220.
- 890 [29] Charpin L., Ehrlacher A. (2014). Micro-poro-mechanics study of anisotropy  
of ASR under loading. *Cement and Concrete Research*. 63.  
<https://doi.org/10.1016/j.cemconres.2014.05.009>.
- [30] Sedran T., De Larrard F. (1994). Un logiciel pour optimiser la granularité des  
matériaux de Génie Civil. *Bulletin des Laboratoires des Ponts et Chaussées*.  
895 194. pp. 87-93.
- [31] Morenon P., Multon S., Sellier A., Grimal E., Hamon F., Kolmayer P. (2019).  
Flexural performance of reinforced concrete beams damaged by Alkali-Silica  
Reaction Flexural performance of reinforced concrete beams damaged by  
Alkali-Silica Reaction. *Cement and Concrete Composites*. 104.
- 900 [32] Institution of Structural Engineers. (1992). *Structural effects of Alkali-Silica  
Reaction: Technical Guidance on the Appraisal of existing structures*, London:  
The Institution.
- [33] Pavoine A., Divet L., Fenouillet S. (2006). A concrete performance test for  
delayed ettringite formation: Part II. Validation. *Cement and Concrete*  
905 *Research*. 36. pp. 2144–2151.